

Supplementary Materials for

A cascade of phase transitions in an orbitally mixed half-filled Landau level

Joseph Falson*, Daniela Tabrea, Ding Zhang, Inti Sodemann, Yusuke Kozuka, Atsushi Tsukazaki, Masashi Kawasaki, Klaus von Klitzing, Jurgen H. Smet*

*Corresponding author. Email: j.falson@fkf.mpg.de (J.F.); j.smet@fkf.mpg.de (J.H.S.)

Published 14 September 2018, *Sci. Adv.* **4**, eaat8742 (2018)
DOI: 10.1126/sciadv.aat8742

This PDF file includes:

Section S1. Further discussion on the ground states

Section S2. Candidate phases

Fig. S1. Observed sequence of states at filling fraction $\tilde{\nu} = 3/2$, which corresponds to a total filling $\nu = 5/2$.

Fig. S2. Continuous depolarization in the auxiliary problem of a two-component half-filled $N = 0$ LL.

Fig. S3. Parameters of samples as a function of charge carrier density.

Fig. S4. Summary of the transitions at $\nu = 5/2$ as a function of n for multiple samples for $1/\cos\theta$.

Fig. S5. Extended data set from Fig. 1.

Fig. S6. Mapping of magnetotransport of sample b around $\nu = 5/2$.

Fig. S7. Temperature-dependent magnetotransport of the ICP1 phase.

Fig. S8. Temperature dependence of anisotropy.

Fig. S9. Map of the hysteresis in the data presented in Fig. 3D at $T = 90$ mK in R_{xy} .

Fig. S10. Analysis of exchange energy corrections to single-particle level crossings.

References (43–46)

Section S1. Further discussion on the ground states

General considerations

To understand the physics near the crossing of $N = 0\downarrow$ and $N = 1\uparrow$, we consider an ideal limit with only these two levels and any other Landau levels neglected. It is convenient to define a filling factor of these two components, $\tilde{\nu}$, which is related to the total filling factor simply by $\nu = 1 + \tilde{\nu}$, and that ranges from $0 \leq \tilde{\nu} \leq 2$. The region that we have focused on experimentally is $1 \leq \tilde{\nu} \leq 2$, and in particular $\nu = 5/2$ corresponds to $\tilde{\nu} = 3/2$.

In the limit under consideration, the Hamiltonian can be taken to have two parts: (a) a single particle splitting term, and (b) a pure interaction term. We call Δ the splitting between these levels. This splitting is understood to include exchange corrections from the fully occupied Landau levels. In the ideal limit in which Landau level mixing can be neglected, we can project the interacting Hamiltonian into the two level system. The single particle energy of the partially filled $N = 1\uparrow$ will acquire a correction due to its exchange interactions with the fully occupied $N = 0\uparrow$ level, however the $N = 0\downarrow$ single particle energies receive no exchange corrections. Therefore in the limit of no Landau level mixing the effective single particle splitting between $N = 1\uparrow$ and $N = 0\downarrow$ is

$$\Delta = E_1 - E_0 = \hbar\omega_c + \frac{e^2}{\epsilon l} \epsilon_e(1) - E_Z \quad (2)$$

Where $\epsilon_e(1) \approx -0.63$ (24), $\epsilon = 8.5\epsilon_0$ is the dielectric constant and $l = \sqrt{\hbar/eB_p}$ the magnetic length. The effective band mass of ZnO is $0.3m_0$, but is strongly renormalized when reducing n (42). We note that the conducting interface is induced without the intentional incorporation of remote ionized impurities and is buried approximately 500 nm beneath the wafer surface and therefore we expect interactions to be screened isotropically by the surrounding intrinsic or lightly Mg-doped ZnO crystal. The full-width at half-maximum of the 2DES wavefunction is calculated to be between 5-6 nm for the range of investigated heterostructures (43). The Hamiltonian includes also Coulomb interactions projected into these two Landau levels in addition to this single particle splitting. Consider an anti-unitary particle-hole conjugation, C , implemented as follows

$$C c_{nm}^\dagger C^{-1} = c_{nm}, C i C^{-1} = -i \quad (3)$$

This operation maps states with fillings $\tilde{\nu} \rightarrow 2 - \tilde{\nu}$ and reverses the splitting $\Delta \rightarrow -\Delta$ while leaving the interacting part of the Hamiltonian invariant. We are focusing only in the region $1 \leq \tilde{\nu} \leq 2$, and hence we cannot use this operation to relate different fillings within this range. However, the existence of this mapping makes convenient to often describe our states as states of holes, with a hole filling defined as $\nu_h = 2 - \tilde{\nu}$.

The total number of particles in each component is conserved exactly due to conservation of spin (because of the smallness of the spin orbit coupling effects in ZnO), which is an important difference with respect to the case of bilayer graphene. The ground state at any value of Δ has a well-defined polarization given by

$$p \equiv \frac{\tilde{\nu}_0 - \tilde{\nu}_1}{\tilde{\nu}_1 + \tilde{\nu}_0} \quad (4)$$

One key question is the dependence of p as a function of Δ . The answer to this question depends on the filling factor. At the level of Hartree-Fock theory at total filling $\tilde{\nu} = \tilde{\nu}_1 + \tilde{\nu}_0 = I$, one obtains a first-order Ising transition with no intermediate coherence, namely, $p = -1$ for $\Delta < 0$ and $p = +1$ for $\Delta > 0$. However, whether a sudden or gradual reversal of polarization occurs at fractional fillings away from $\tilde{\nu} = 1$ is an unresolved theoretical question.

Our experiment has found at $\tilde{\nu} = 3/2$ a non-trivial sequence of phase transitions as a function of Δ which is experimentally modified by changing θ , as summarized in Fig. S1. We currently have no direct way of measuring p , but we believe such non-trivial sequence is compatible with a partial depolarization taking place in stages as the two levels cross, as we argue in more detail below. Observations of a gradual depolarization in the related system of bilayer graphene were reported in (5).

Section S2. Candidate phases

We begin by labeling the states we have experimentally encountered at total filling $\tilde{\nu} = 3/2$ as we tune the value of Δ by tilting the sample. At low tilts, where the $N = 1\uparrow$ character is favored, we encounter an incompressible state that we label ICP1. As Δ is decreased this state disappears into an isotropic compressible state that we label CP1. Then, for a narrow but finite range of Δ , a second incompressible state appears and we

label it ICP2. This incompressible state then transitions into a strongly anisotropic compressible state that we label ACP. Finally, at larger Δ , this state transitions into a second compressible phase that we label CP2 (see Fig. S1).

The first important consideration is to establish a correspondence between the locations of these different phases relative to the ideal point at which the single particle splitting, Δ , vanishes. We associate the location of this point in experiment with the peak obtained from the hysteretic sweeps of the magnetoresistance at high temperatures, depicted in Fig. 3E, across $1 \leq \tilde{\nu} \leq 2$. The ICP2 phase occurs in the vicinity of such high temperature features, and therefore we locate the ICP2 phase to be in the vicinity of the single particle level crossing, as depicted in Fig. S1.

We will now list a series of possible candidate phases and their properties and discuss which of these phases are consistent with those we are observing. At filling $\tilde{\nu} = 3/2$, a large class of states can be considered by employing the composite fermion picture. We begin with phases that have a composite Fermi liquid (CFL) nature. Since we are considering a two-component system it is possible to have CFL phases with two Fermi surfaces (in analogy to the $N = 0$ Landau level in the limit of small Zeeman splitting) (32, 33, 44). We label these phases as CFL(ν_{h0} ; ν_{h1}) by the corresponding partial hole fillings of the $N = 0/1$ components. These phases have a compressible nature, featuring a finite metallic-like resistivity $\rho_{xx} \neq 0$ and an unquantized Hall resistivity ρ_{xy} .

These phases are natural candidates for the CP1 and CP2 phases we observe. The CFL(1/2,0) is undoubtedly a good candidate description of the CP2 phase we are observing, since this phase appears in the limit of large splitting and when the chemical potential lies in the $N = 0$ LL. The phase CP1, on the other hand, is more difficult to understand. It nominally appears in the region in which the chemical potential lies in the $N = 1 \uparrow$ level but only within a range that lies in the vicinity of the level crossing. It is possible that this phase corresponds to a state with two Fermi surfaces, namely CFL(ν_{h0} , ν_{h1}) with $\nu_{h0,h1} \neq 0$. Such two component states have been considered theoretically in Refs. (13) and (14). Moreover a study of the bilayer graphene system that also realizes an analogous level crossing between $N = 0$ and $N = 1$ Landau levels, reported a gradual depolarization of the two components at half-filling and also considered the above states as partially polarized candidate phases (5). We would like to offer an

argument for why they might be energetically plausible in the present context. To do so, we consider an auxiliary problem in which we have a system of two levels with opposite spins but the same orbital character $N = 0$. It is well established experimentally and theoretically that at $\tilde{\nu} = 1/2$ such a system is described by an unpolarized Fermi sea in which both components have the same density in the limit of $\Delta = 0$. It is also well established that the polarization, p , as a function of Δ in such a system is a continuous function of Δ that interpolates between the two fully polarized states at large $|\Delta|$ as depicted in Fig. S2. Now, the problem we are considering can be viewed as one that is perturbed away from this auxiliary problem by tuning the Haldane pseudopotentials for a single component from the values corresponding to $N = 0$ into those of $N = 1$. Such perturbation is by no means small, but one could imagine that the correlations that help to establish the continuous depolarization auxiliary problem could survive against such perturbation. More physically, we can say that there is a composite fermion kinetic energy loss associated with depolarizing the two component Fermi sea, that competes with other potential energy gains such as the correlation energy gained by polarizing into a single component and pairing into the Moore-Read state. The question of how such energy competition is settled is very non-trivial but could be addressed in future numerical studies.

Another class of closely related states are those obtained by pairing of the composite fermions in a CFL($\tilde{\nu}_0, \tilde{\nu}_1$) phase. These states will be incompressible in the sense that they will feature a vanishing ρ_{xx} and a quantized $\rho_{xy}[h/e^2] = 2/5$ at low temperatures. This is true even if only one of the two components forms a paired state while the other remains in a Fermi surface state, such as in the recently proposed Z_2 exciton metal (13, 14). In the case of bilayer graphene, the crossing involves the valley degree of freedom and therefore valley is a conserved quantum number across the level crossing, while in ZnO it is electron spin. This property can be economically understood by appealing to the parton construction of the composite fermion states (see e.g. 45) in conjunction with the Ioffe-Larkin rule (46), according to which we view the physical electron as

$$c_N^\dagger = \psi_N^\dagger b^\dagger, N = \{0 \uparrow, 1 \downarrow\} \quad (5)$$

where b^\dagger is a boson that carries physical charge 1 and ψ_N^\dagger are charge neutral composite fermions that carry the Landau level flavor degree of freedom N . The boson forms a $\nu = 1/2$ Laughlin state, and the fermions can form states at effective zero magnetic field such as Fermi surfaces or paired states. According to the Ioffe-Larkin rule the physical resistivity is obtained by adding the resistivity tensors of the partons as follows:

$\rho = \rho_b + \rho_\psi$. On the one hand the resistivity tensor of the bosonic sector is simply the one of the Laughlin state at $\nu = 1/2$. The fermions will have a resistivity that would correspond to a state at effective zero magnetic field. If the fermions are paired the net resistivity will vanish. This is true even if only one component is paired and the other forms a Fermi surface. Such case would be analogous to computing the net resistivity of a bilayer system in which one layer is in a superconducting state and the other in an ordinary metal. The current will be shunted by the superconducting component and hence the net resistivity vanishes. This scenario corresponds to the case of the Z_2 exciton metal proposed in Ref. (13).

There is a plethora of states that one could obtain by considering different specific pairing channels of composite fermions. From the point of view of electric transport all of them will be candidates for the ICP1 and ICP2 phases. The most natural candidate state for the ICP1 phase is undoubtedly the Moore-Read state (or its particle-hole conjugate) which can be viewed as $p + ip$ weakly-paired states of the CFL(0,1/2), since this is the leading candidate to explain the even denominator state of an isolated $N = 1$ Landau level. Also, it is possible that near the boundary of the ICP1 phase and the CP1 phase the partially polarized Z_2 exciton metal proposed in Ref. (13) might be realized, since this state would display essentially similar features in charge transport as the Moore-Read state.

The ICP2 phase is much more non-trivial to understand, but we would like to elaborate on a few potential candidates. One possibility is again that this phase corresponds also to the Moore-Read state. Some studies have found that the Moore-Read state is enhanced near level crossings of sub-bands before suddenly disappearing (34). In light of this, an interesting possibility is that the Moore-Read state never truly disappears but its gap has a very non-monotonic behavior as a function of the level splitting. The phase we call CP1 in an ideal limit may simply be a weaker version of the Moore-Read state with a gap that has been washed out by disorder and temperature effects, which has a sudden revival near the

level crossing. Another interesting possibility is that this state is a paired state that is sharply distinct from the Moore-Read state. Since this state occurs near the coincidence point of the two levels, a natural alternative candidate would be the analogue of the Halperin-331 state which can also be understood as a paired state in the two component triplet $p + ip$ channel (8) and has equal density for both components.

Finally, we discuss the strongly anisotropic state ACP that appears in between the incompressible state ICP2 and the compressible CP2 state. A natural candidate for a state with strong transport anisotropy in a half-filled Landau level is the stripe phase. This phase arises more naturally in higher Landau levels, but it is not un-common for it to be stabilized in the $N = 1$ Landau level since it is understood to be in close energetic competition with the Moore-Read state (40). The feature that makes its appearance unexpected in the current case is that the phase seems favored near the level crossing with a $N = 0$ Landau level. One interesting scenario is that this phase corresponds to a state with coherence between the $N = 0\downarrow$ and $N = 1\uparrow$ levels. As these orbitals carry different orbital angular momentum, a coherent superposition would break inversion and rotation symmetries, rendering the state with nematic and ferroelectric characteristics, explaining its anisotropic nature. In addition the opposite spin would endow the state with a finite magnetization in the plane orthogonal to the spin quantization axis dictated by the Zeeman energy. Proposals for related ferroelectric states in bilayer graphene have been made at integer filling factors (19) but there are to the best of our knowledge no studies addressing their energetic feasibility for half-filled Landau levels.

While the above theoretical considerations have neglected the effects of inter-LL mixing, we note that the ratio of the Coulomb energy to cyclotron gap, κ , at $\nu = 5/2$ is large ($\kappa \geq 5$) in all the samples investigated. When it is large, the effect of Landau level mixing is often incorporated by replacing the static coulomb interaction with the RPA statically screened form (29, 30). However, in the present case such an approach possibly needs to be upgraded in order to capture the changes in screening that happen near the level crossing. One underlying aspect of this is the sudden Pauli blocking of certain virtual transitions from the occupied levels. This is expected to both quantitatively modify the energy gaps of the states observed and also impose particle-hole symmetry breaking terms (26-28). While strenuous to handle theoretically, this is expected to lift the degeneracy of the Pfaffian and anti-Pfaffian phases in the context of the even-denominator FQH states.

Future experimental work will focus on detecting signatures which may categorically identify the observed ICP1 and ICP2 phases and to understand the differences between the cascade observed in this work and the closely related level crossings reported in Refs. (5, 6).

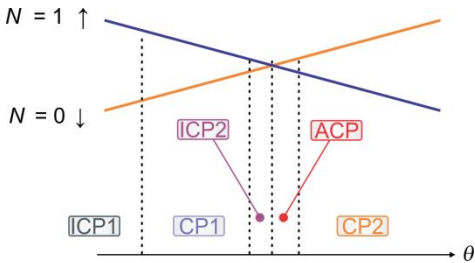


Fig. S1. Observed sequence of states at filling fraction $\tilde{\nu} = 3/2$, which corresponds to a total filling $\nu = 5/2$.

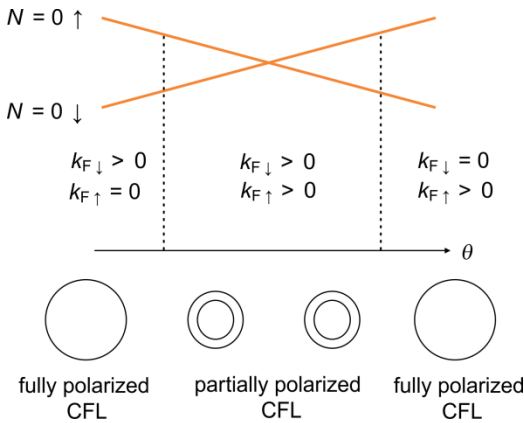


Fig. S2. Continuous depolarization in the auxiliary problem of a two-component half-filled $N = 0$ LL.

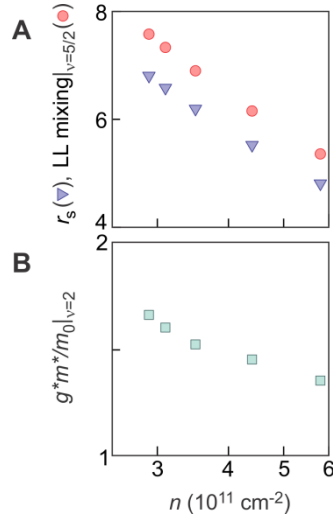


Fig. S3. Parameters of samples as a function of charge carrier density. (A) $r_s = \left(\frac{e^2 m^*}{4\pi\hbar^2 \epsilon \sqrt{\pi n}} \right)$ and LL mixing at $\nu = 5/2$ ($E_c/E_{cyc} = 16.6/\sqrt{B}|_{\nu=5/2}$). The effect of LL mixing on the stability of FQH features has been discussed in (29) and (30). **(B)** g^*m^*/m_0 . We note the bulk parameters are $m^* = 0.3m_0$, $g = 2$ and dielectric constant $\epsilon = 8.5\epsilon_0$.

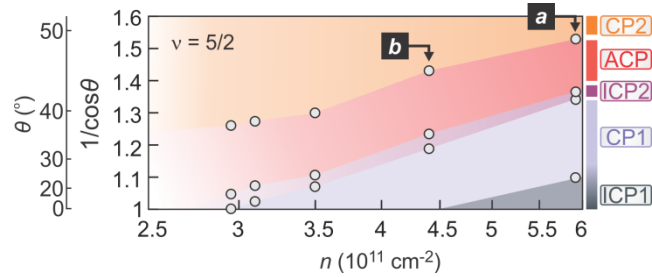


Fig. S4. Summary of the transitions at $\nu = 5/2$ as a function of n for multiple samples for $1/\cos\theta$.

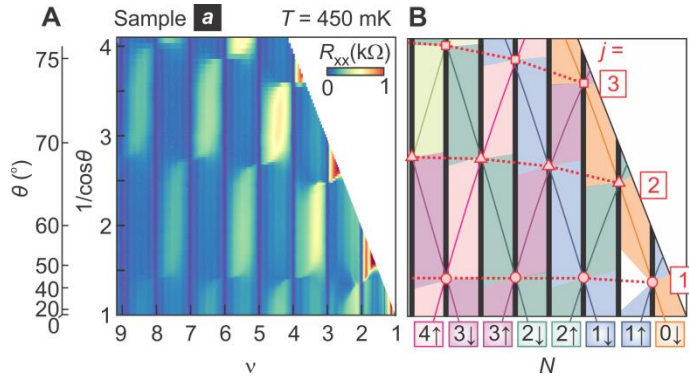


Fig. S5. Extended data set from Fig. 1. (A) $T = 450$ mK mapping of the magnetotransport of sample *a* ($n = 5.8 \times 10^{11} \text{ cm}^{-2}$) with (B) displaying the corresponding orbital quantum number and spin projection of the partially filled level. The first ($j = 1$, circles), second ($j = 2$, triangles) and third ($j = 3$, squares) coincidence positions are interpolated by dotted lines. This representation highlights that the j coincidence positions slip to lower θ as ν is made small, which is attributed (23) to a polarization dependent contribution to g^*m^*/m_0 .

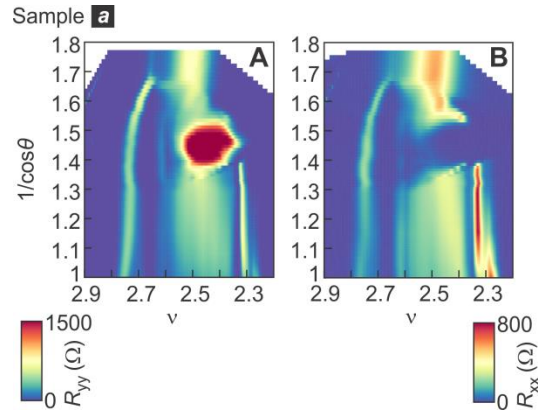


Fig. S6. Mapping of magnetotransport of sample b around $\nu = 5/2$. Map of (A) R_{xx} and (B) R_{yy} around $\nu = 5/2$ for sample *b* at $T \sim 30$ mK up to high field ($B = 18$ T). The ACP phase is completely resolved, along with the CP2 phase at higher θ . Data shown in the main manuscript were taken in a $B = 15$ T, $T < 20$ mK cryostat.

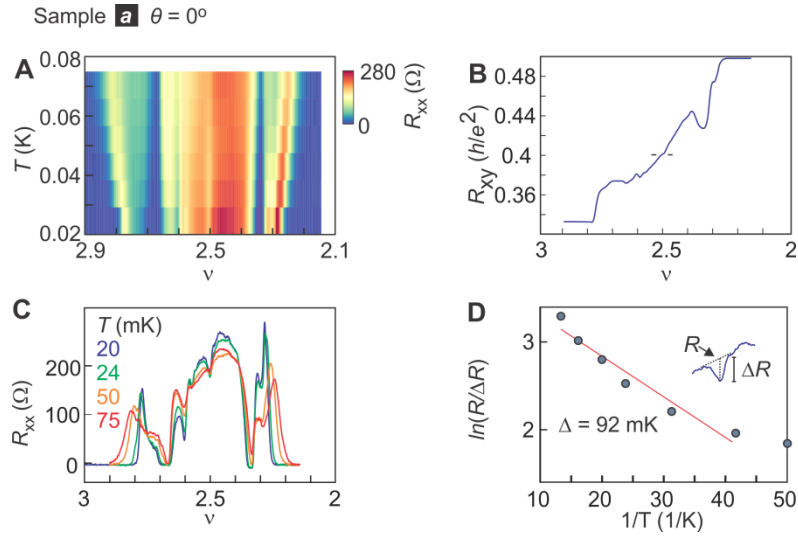


Fig. S7. Temperature-dependent magnetotransport of the ICP1 phase. (A)

Magnetotransport as a function of T when $\theta = 0^\circ$ for sample *a*. **(B)** R_{xy} at base temperature. **(C)** Individual line traces of the temperature dependent R_{xx} data. **(D)** Arrhenius plot of $R/\Delta R$ of the $\nu = 5/2$ resistance. The activation energy is estimated through $R/\Delta R \propto \exp(-\Delta_{\nu=5/2}/2T)$.

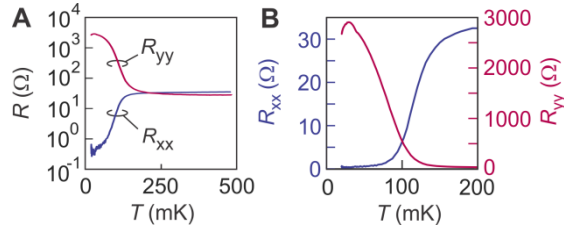


Fig. S8. Temperature dependence of anisotropy. Temperature dependence of the anisotropic phase for $1/\cos\theta = 1.33$ and $\nu = 2.4$ for two orthogonal crystal directions on **(A)** log and **(B)** linear scale.

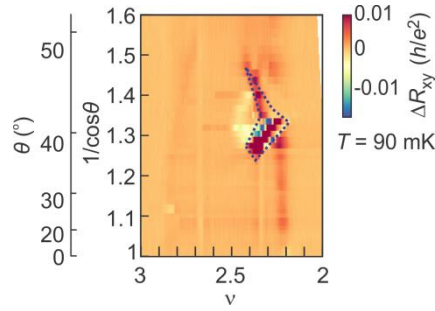


Fig. S9. Map of the hysteresis in the data presented in Fig. 3D at $T = 90$ mK in R_{xy} . The dotted blue region frames the hysteretic region that is incorporated into Fig. 4A.

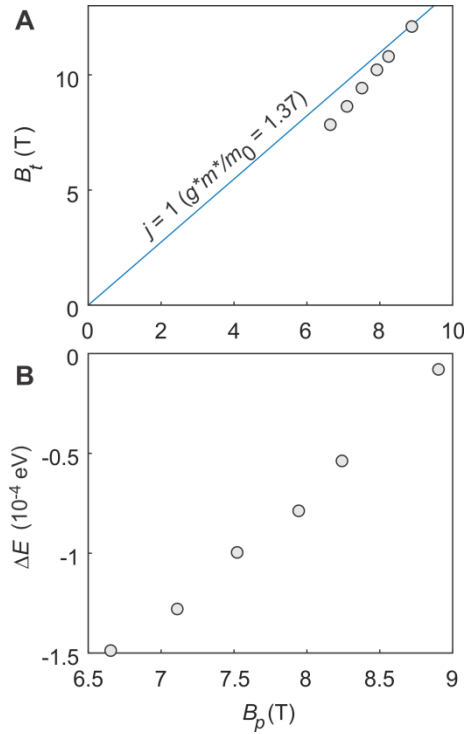


Fig. S10. Analysis of exchange energy corrections to single-particle level crossings. (A) (Line) slope of the $j=1$ coincidence assuming a constant g^*m^*/m_0 . (Open circles) Experimentally observed maxima in hysteresis of the resistance in Fig. 3E in the B_p - B_t plane taken on sample b . (B) The deviation between these provides an estimate of the exchange energy corrections to the single particle energy levels.